Supporting information

Fabrication of magnetic amino-functionalized nanoparticles for *S*-arylation of heterocyclic thiols

Yanhong Liu,[abc] Lincheng Zhou,*[a] Xinping Hui,*[a] Zhenwen Dong,[a] Hao Zhu,[a] Yanming Shao[a] and Yanfeng Li[a]

[a] *College of Chemistry and Chemical Engineering, Lanzhou University, Lanzhou 730000, PR China*

[b] *Key Laboratory of Petroleum Resources Research, Institute of Geology and Geophysics, Chinese Academy of Sciences, Lanzhou 730000, PR China.*

[c] *University of Chinese Academy of Sciences, Beijing 100049, PR China.*

Contents

1. Chemicals and instrumentation

Ferric acetylacetonate, dibenzyl ether, oleylamine, polyethylene imine-600 (PEI-600) (Fig. S1) were purchased from Sigma Aldrich. Aminopropyltriethoxysilane (APTES) was purchased from Nanjing Xinhuai Technology Co. Ltd.. 3-Isocyanatopropyltriethoxysilane (ICPTS) was purchased from J & K Scientific Ltd.. Copper (I) iodide was commercially available. 4,5-Diphenyl-1,2,4-triazol-3-thione was prepared according to literature method.[1] DMF, dichloromethane, toluene, tetrahydrofuran, triethylamine and acryloyl chloride were purified according to standard methods. All experiments were carried out under nitrogen atmosphere. TLC plates were used to track reaction.

NMR spectra were recorded on Varian Mercury-400 MHz or Bruker AM-400 spectrometer and chemical shifts were expressed in units (ppm) relative to the TMS (^{1}H NMR) or to the solvent (^{13}C NMR). IR spectra were performed with Nicolet NEXUS 670 FT-IR instrument. Elemental analyses were obtained on Elementar vario EL. X-Ray diffraction (XRD) spectra were obtained using a Rigaku D/MAX-2400 X-ray powder diffractometer. The morphology of the catalysts was studied by transmission electron microscopy (FEI Tecnai G20). Field dependent magnetization curves were determined by a LAKESHORE-7304 vibrating sample magnetometer (VSM). Surface composition of the ligands was obtained by analyzing XPS data in Thermo ESCALAB 250Xi X-ray photo-electron spectrometer.

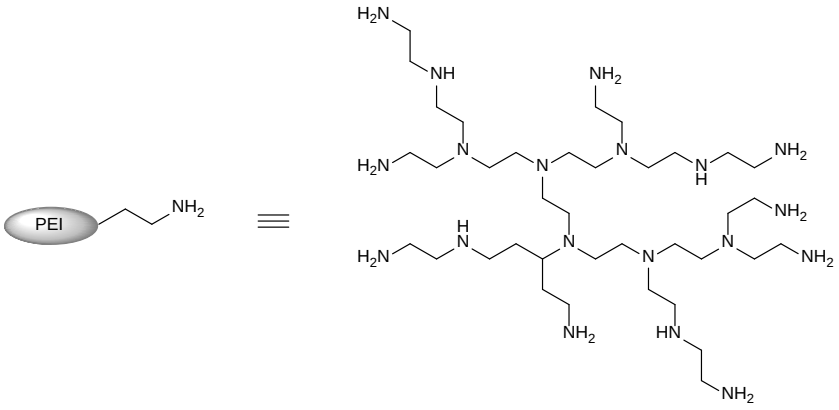

Fig. S1 The structure of polyethylene imine (PEI).

2. Experimental procedures

Preparation of $CoFe_2O_4$-NH_2 nanoparticles (MNL A).[2] To a solution of anhydrous $FeCl_3$ (0.683 g, 4.2 mmol) and $CoCl_2$•$6H_2O$ (0.576 g, 2.1 mmol) in ethylene glycol (30 mL) was added sodium

acetate (1.5 g) and the mixture was stirred for 30 min at 80°C. Then the solution was refluxed with ethanolamine (15 mL) for 6 h. It was cooled to room temperature. The $CoFe_2O_4$-NH_2 particles were separated magnetically and washed with ethanol (4×5 mL), dried at 40°C under vacuum for 12 h and black powder (MNL **A**) was obtained. The nitrogen content was 0.90 wt%.

Preparation of Fe_3O_4 nanoparticles.[3] $Fe(acac)_3$ (0.706 g, 2 mmol) was dissolved in benzyl ether (10 mL) and oleylamine (10 mL). The solution was dehydrated at 110°C for 1 h under nitrogen atmosphere to wipe out low boiling point substances, then quickly heated to 300°C and kept at this temperature for 2 h. The mixture was cooled to room temperature and the Fe_3O_4 NPs were recovered magnetically after addition of ethanol (60 mL) and washed with ethanol (4×5 mL). Ferrite was characterized by transmission electron microscopy (TEM) and X-ray diffraction (XRD). The Fe_3O_4 NPs were dispersed in dichloromethane (30 mL) and then used for further chemical modification.

Preparation of Fe_3O_4@$Si(CH_2)_3NH_2$ (MNL B). Fe_3O_4 magnetic nanoparticles (about 0.50 g) were refluxed with 3-aminopropyltriethoxysilane (0.5 mL) in dry toluene (50 mL) under nitrogen atmosphere for 3 days.[4] The solid was separated magnetically and washed with ethanol (4×30 mL). The resulting powder (MNL **B**) was dried at 40°C under vacuum for 12 h. The nitrogen content was 3.80 wt%.

Preparation of Fe_3O_4@$Si(CH_2)_3NHC(O)(CH_2)_2$PEI (MNL C). MNL B (0.050 g) was dispersed in dry dichloromethane (2.0 mL), and cooled in an ice-water bath. Triethylamine (24 μL, 0.17 mmol) was added and the mixture was stirred for 30 min. Then, acryloyl chloride (11 μL, 0.14 mmol) was added dropwisely, and the mixture was stirred at room temperature for 48 h. It was washed with DI H_2O (3×5 mL) and acetone (3×5 mL). The resulting product was dried at 40°C under vacuum for 5 h, then dispersed in methanol (2.0 mL), and mixed with PEI-600 (30 μL) at room temperature for 2 days.[4] The solid was separated by a magnetic field and washed with ethanol (5×3 mL). The resulting product was dried under vacuum for 12 h. The nitrogen content was 3.20 wt%.

Preparation of Fe_3O_4@Si$(CH_2)_3$NHC(O)PEI (MNL D). Fe_3O_4 magnetic nanoparticles (100 mg) were refluxed with 3-(triethoxysilyl)propyl isocyanate (50 μL) in dry toluene (5 mL) under nitrogen atmosphere for 3 days.[5] The nanoparticles were washed with dry ethyl acetate (3×10 mL) and petroleum ether (3×10 mL). The resulting product was dried under vacuum for 5 h, then dispersed in dry acetonitrile (4 mL) and refluxed with PEI-600 (40 μL) for 24 h. The solid was separated by a magnetic field and washed with DI H_2O (3×8 mL) and ethanol (3×8 mL). The resulting product was then dried at 40°C under vacuum for 12 h. The nitrogen content was 2.80 wt%.

3. Characterization of material

The XRD pattern of MNL **A** (Figure S2a) was matched perfectly to the expected cubic spinel structure of $CoFe_2O_4$. The position and relative intensities were also consistent with those from JCPDS card (22-1086) for $CoFe_2O_4$. In the XRD patterns of MNLs **B**, **C** and **D** (Fig. S2b, S2c and S2d), the peaks at 2θ = 30.7°, 35.6°, 42.9°, 53.4°, 57.3° and 62.8° were consistent with standard Fe_3O_4 peaks (JCPDS 19-629).

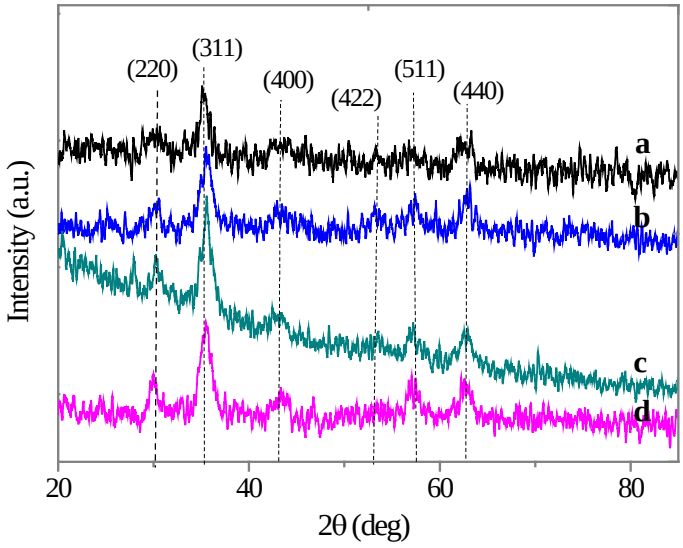

Fig. S2 X-Ray diffraction patters of MNLs **A** (a), **B** (b), **C** (c) and **D** (d).

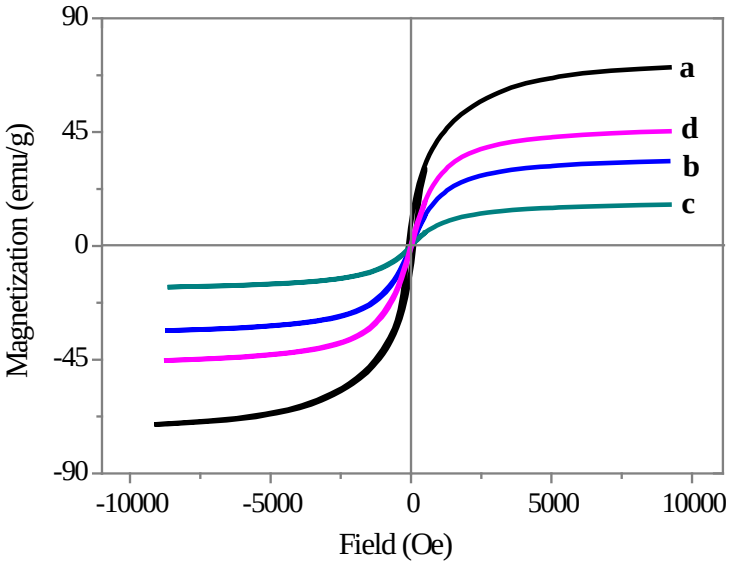

Fig. S3 Hysteresis loops of MNLs **A** (a), **B** (b), **C** (c) and **D** (d).

In the IR spectra (Fig. S4) of the nanoparticles, the appearance of a characteristic band at 595 cm^{-1}, corresponding to the stretch vibration of the Fe–O group, confirmed the existence of the magnetic core. The C–H stretch was visible at 2900 cm^{-1}. The N–H stretch at 1640 cm^{-1} and the C–N stretch at 1340 cm^{-1} provided evidence of surface amine-functionalization. Also, the C=O peaks of MNLs **C** and **D** were observed at 1711 cm^{-1} and 1558 cm^{-1}, respectively.

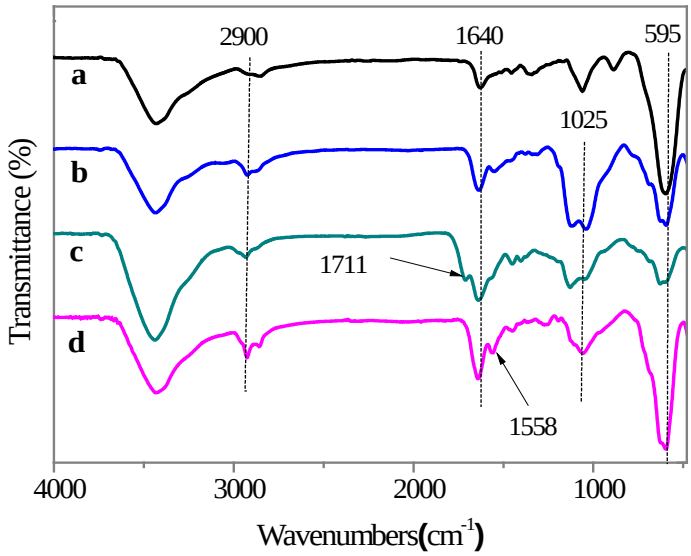

Fig. S4 Infrared spectra of MNLs **A** (a), **B** (b), **C** (c) and **D** (d).

For the freshly synthesized MNL **B** and MNL **B** after the 5th run, the powder X-ray diffraction analysis exhibited identical peaks for both of them, which were compared with the standard Fe_3O_4 peaks (JCPDS 19-629) (Fig. S5a). The typical hysteresis loops at room temperature (300 K) identified the super-paramagnetic nature of both the fresh and recovered MNL **B**. Ms values for both the freshly synthesized MNL **B**, and MNL **B** after the 5th run, were 33.5 emu·g^{-1} and 33.4 emu·g^{-1} (Fig. S5b), respectively. This decrease in Ms value was too small to affect magnetic separation. The peaks in the IR spectra (Fig. S5c) indicated that the material exhibited good stability under the described reaction conditions.

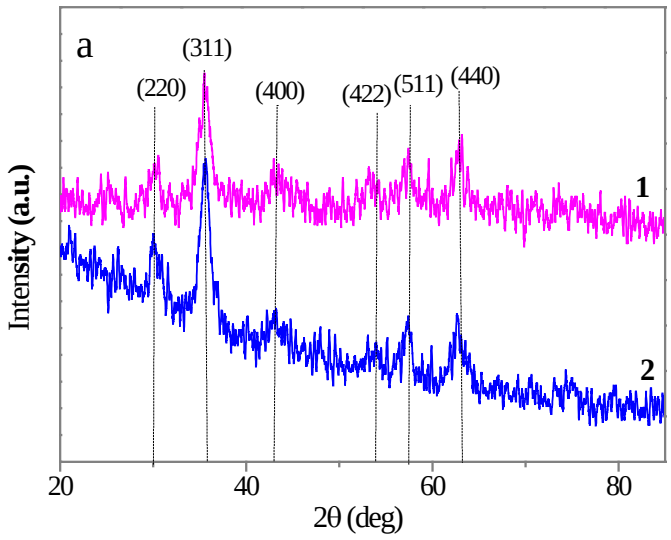

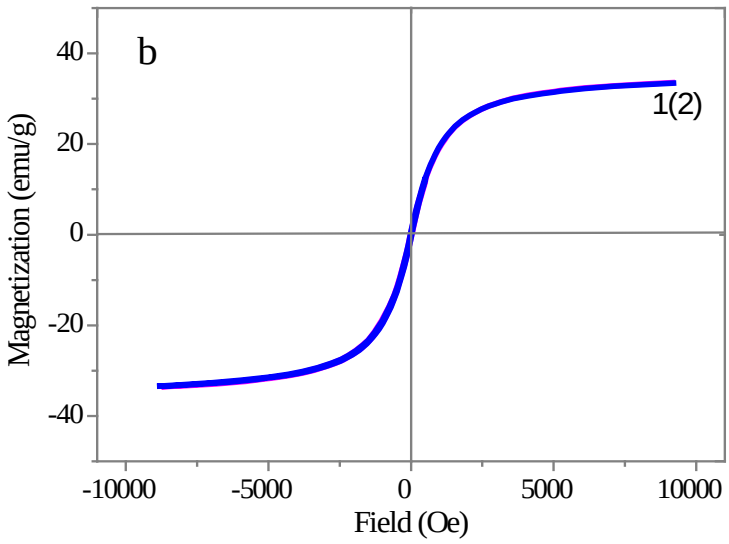

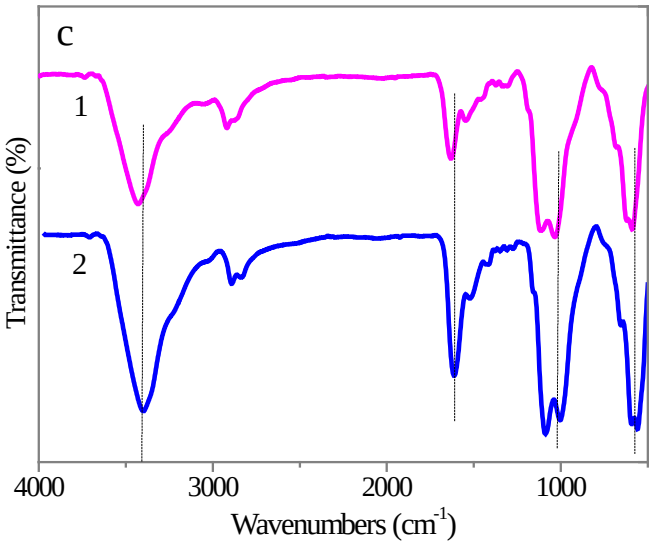

Fig. S5 X-Ray diffraction patterns (a), hysteresis loops (b), and infrared spectrum (c) of nano-ligands. Freshly synthesized MNL **B** (1) and MNL **B** after the 5th run (2).

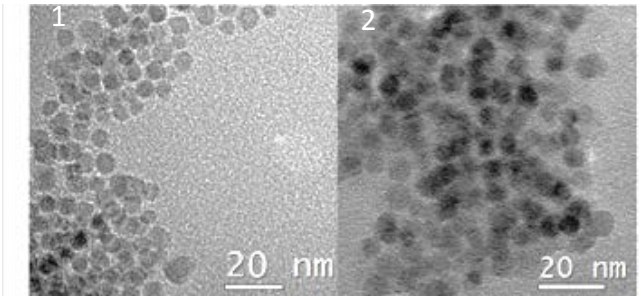

Fig. S6 TEM of freshly synthesized MNL **B** (1) and MNL **B** after the 5th run (2).

The XPS spectra of freshly synthesized MNL **B**, and MNL **B** after the 5th run (Fig. S7) indicated no obvious differences, while the XPS of Fe 2p from the Fe_3O_4 nanoparticles (Fig. S8a) demonstrated the simultaneous existence of Fe 2p 1/2 (723.5 eV) and Fe 2p 3/2 (709.3 eV), which were close to the standard data reported for Fe_3O_4. The high-resolution C 1s spectrum was shown in Fig. S8b. The carbon peak observed at 284.9 eV was close to the binding energy (Eb) of aliphatic carbon (C–C or C–H), and it likely originated from the long alkyl chain of APTES. The XPS of the O 1s regions for both fresh and recovered MNL **B** in Fig. S8d indicated the existence of O 1s (528.9 eV) from the Fe_3O_4 nanoparticles and O 1s (531.1 eV) from the Si–O group, respectively. The N 1s signal of freshly synthesized MNL **B**, observed at 398.3 eV, corresponded to the binding energy (Eb) of aliphatic amine (N–C, N–H) (Fig. S8c). After the 5th run, this value increased approximately 1.3

eV due to the coordination interaction between copper and the nitrogen atom. The peaks for Cu 2p 1/2 (951.7 eV) and Cu 2p 3/2 (932.4 eV) (Fig. S8f) were close to the standard data of Cu^0, which results from reduction of Cu(I). The existence of Cu 2p was consistent with an increase of N 1s binding energy, which was consistent with the formation of Cu^0 nanoparticles.

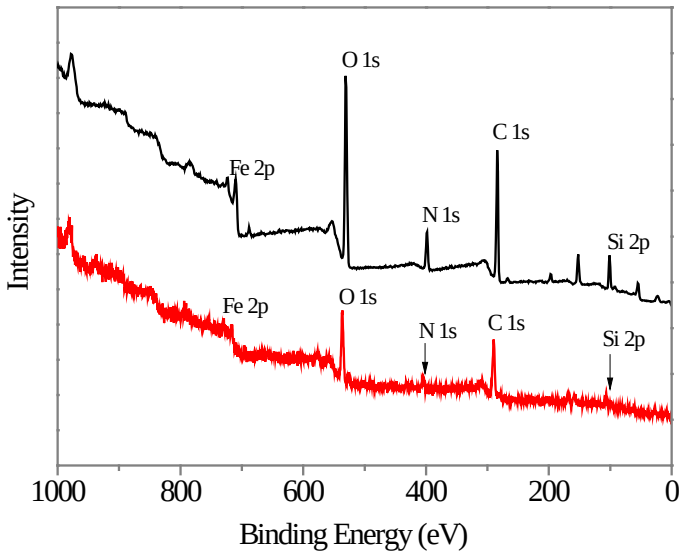

Fig. S7 Survey XPS spectra of freshly synthesized MNL **B** (—) and MNL **B** after the 5th run (—).

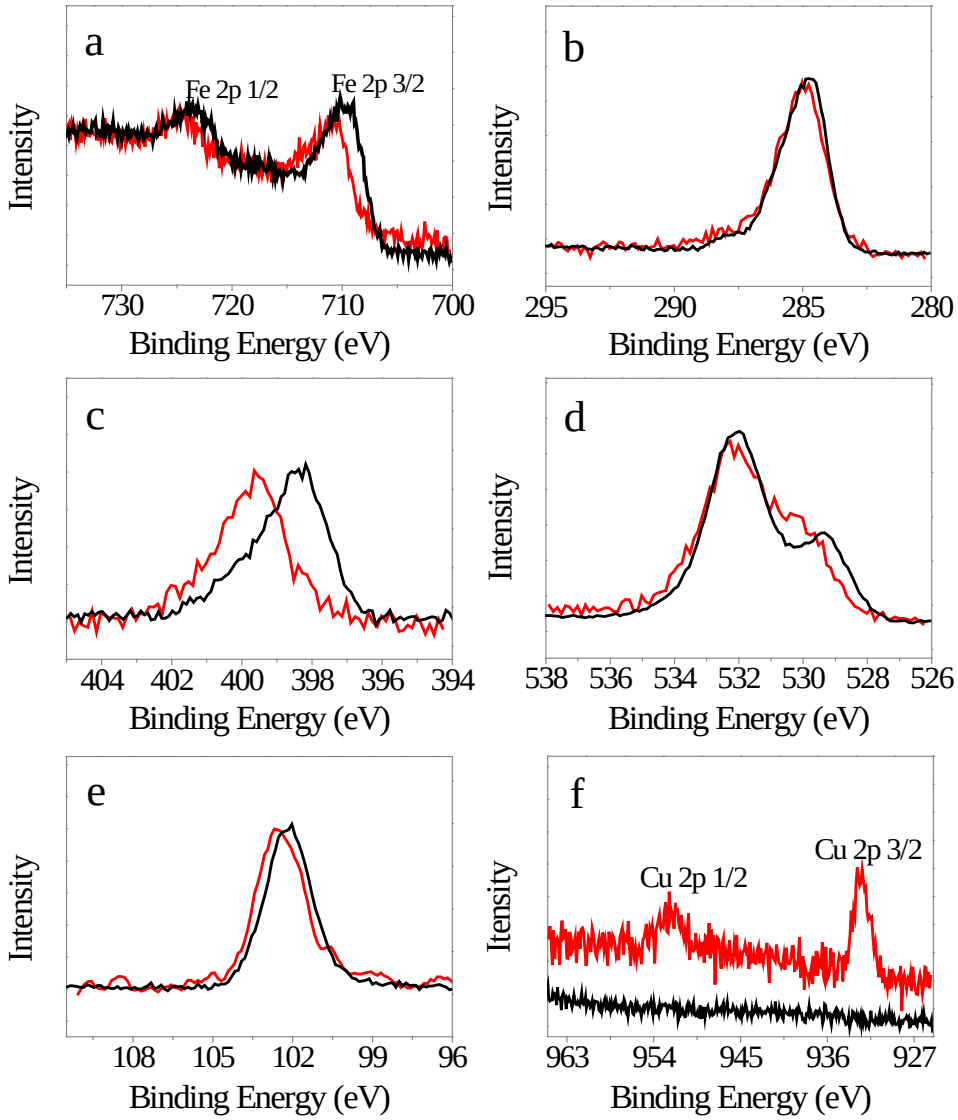

Fig. S8 Comparison of the regions for Fe 2p (a), C 1s (b), N 1s (c), O (1s) (d), Si 2p (e) and Cu 2p (f), respectively. Freshly synthesized MNL **B** (—), and MNL **B** after the 5th run (—).

3. Characterization of Compounds

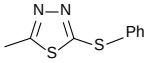

2-Methyl-5-(phenylthio)-1,3,4-thiadiazole (Table 3, entry 1)[6]. ^{1}H NMR (400 MHz, $CDCl_3$) δ: 7.65 – 7.63 (m, 2H, ArH), 7.45 – 7.41 (m, 3H, ArH), 2.68 (s, 3H, CH_3). ^{13}C NMR (100 MHz, $CDCl_3$) δ: 167.58, 166.09, 133.65, 131.03, 129.76, 15.55.

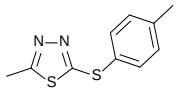

2-Methyl-5-(*p*-tolylthio)-1,3,4-thiadiazole (Table 3, entry 2). ^{1}H NMR (400 MHz, $CDCl_3$) δ: 7.52 (d, *J* = 8.0 Hz, 2H, ArH), 7.22 (d, *J* = 8.0 Hz, 2H, ArH), 2.64 (s, 3H, CH_3), 2.38 (s, 3H, CH_3). ^{13}C NMR (100 MHz, $CDCl_3$) δ: 168.83, 165.50, 140.44, 134.01, 130.53, 127.29, 21.12, 15.45.

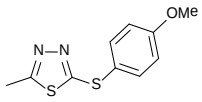

2-[(4-Methoxyphenyl)thio]-5-methyl-1,3,4-thiadiazole (Table 3, entry 3). ^{1}H NMR (400 MHz, $CDCl_3$) δ: 7.54 (d, *J* = 8.8 Hz, 2H, ArH), 6.91 (d, *J* = 8.8 Hz, 2H, ArH), 3.81 (s, 3H, CH_3), 2.60 (s, 3H, CH_3). ^{13}C NMR (100 MHz, $CDCl_3$) δ: 170.46, 165.64, 161.57, 136.62, 121.51, 115.71, 55.64, 15.80.

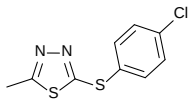

2-[(4-Chlorophenyl)thio]-5-methyl-1,3,4-thiadiazole (Table 3, entry 4). ^{1}H NMR (400 MHz, $CDCl_3$) δ: 7.52 (d, *J* = 8.4 Hz, 2H, ArH), 7.34 (d, *J* = 8.4 Hz, 2H, ArH), 2.65 (s, 3H, CH_3). ^{13}C NMR (100 MHz, $CDCl_3$) δ: 166.78, 165.56, 136.48, 135.11, 130.25, 129.68, 15.92.

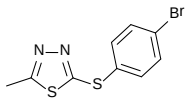

2-[(4-Bromophenyl)thio]-5-methyl-1,3,4-thiadiazole (Table 3, entry 5). ^{1}H NMR (400 MHz, $CDCl_3$) δ: 7.50 (d, *J* = 8.4 Hz, 2H, ArH), 7.45 (d, *J* = 8.8 Hz, 2H, ArH), 2.66 (s, 3H, CH_3). ^{13}C NMR (100 MHz, $CDCl_3$) δ: 166.57, 166.00, 134.91, 132.90, 130.06, 124.34, 15.64.

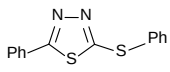

2-Phenyl-5-(phenylthio)-1,3,4-thiadiazole (Table 3, entry 6)[6]. ^{1}H NMR (300 MHz, $CDCl_3$) δ: 7.85 – 7.82 (m, 2H, ArH), 7.72 – 7.70 (m, 2H, ArH), 7.49 – 7.37 (m, 6H, ArH).

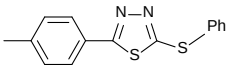

2-(Phenylthio)-5-*p*-tolyl-1,3,4-thiadiazole (Table 3, entry 7)[6]. ^{1}H NMR (400 MHz, $CDCl_3$) δ: 7.74 – 7.68 (m, 4H, ArH), 7.48 – 7.45 (m, 3H, ArH), 7.23 (d, *J* = 8.4 Hz, 2H, ArH), 2.39 (s, 3H, CH_3). ^{13}C NMR (100 MHz, $CDCl_3$) δ: 169.37, 167.43, 138.83, 133.87, 131.77, 130.95, 129.98, 129.87, 129.59, 128.86, 128.03, 124.80, 21.12.

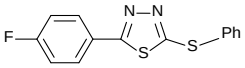

2-(4-Fluorophenyl)-5-(phenylthio)-1,3,4-thiadiazole (Table 3, entry 8)[6]. ^{1}H NMR (400 MHz, $CDCl_3$) δ: 7.84 – 7.81 (m, 2H, ArH), 7.71 – 7.69 (m, 2H, ArH), 7.49 – 7.45 (m, 3H, ArH), 7.14 – 7.10 (m, 2H, ArH). ^{13}C NMR (100 MHz, $CDCl_3$) δ: 168.00, 165.51, 164.31 (d, *J* = 251.0 Hz), 134.13, 130.90, 130.23, 130.04, 129.68 (d, *J* = 9.0 Hz), 126,18 (d, *J* = 3.0 Hz), 116.32 (d, *J* = 22.0 Hz).

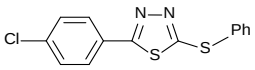

2-(4-Chlorophenyl)-5-(phenylthio)-1,3,4-thiadiazole (Table 3, entry 9)[6]. ^{1}H NMR (400 MHz, $CDCl_3$) δ: 7.77 (d, *J* = 8.8 Hz, 2H, ArH), 7.72 – 7.70 (m, 2H, ArH), 7.50 – 7.47 (m, 3H, ArH), 7.41 (d, *J* = 8.8 Hz, 2H, ArH). ^{13}C NMR (100 MHz, $CDCl_3$) δ: 169.49, 166.55, 162.11, 134.05, 131.46, 130.19, 129.46, 122.72, 114.71, 55.67.

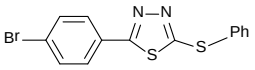

2-(4-Bromophenyl)-5-(phenylthio)-1,3,4-thiadiazole (Table 3, entry 10)[6]. ^{1}H NMR (400 MHz, $CDCl_3$) δ: 7.71 – 7.68 (m, 4H, ArH), 7.55 (d, 2H, *J* = 8.4 Hz, ArH), 7.49–7.44 (m, 3H, ArH). ^{13}C NMR (100 MHz, $CDCl_3$) δ: 168.55, 167.90, 134.20, 132.31, 130.73, 130.31, 130.07, 128.94, 128.73, 125.48.

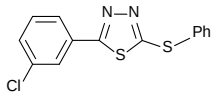

2-(3-Chlorophenyl)-5-(phenylthio)-1,3,4-thiadiazole (Table 3, entry 11)[6]. ^{1}H NMR (400 MHz, $CDCl_3$) δ: 7.83 (s, 1H, ArH), 7.72 – 7.70 (m, 3H, ArH), 7.51 – 7.34 (m, 5H, ArH). ^{13}C NMR (100 MHz, $CDCl_3$) δ: 168.87, 167.22, 134.91, 134.07, 131.19, 130.77, 130.47, 130.21, 129.97, 127.20, 125.60.

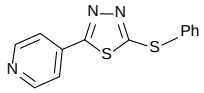

4-(5-(Phenylthio)-1,3,4-thiadiazol-2-yl)pyridine (Table 3, entry 12)[6]. ^{1}H NMR (400 MHz, $CDCl_3$) δ: 8.66 (d, *J* = 4.8 Hz, 2H, ArH), 7.70 – 7.64 (m, 4H, ArH), 7.49 – 7.45 (m, 3H, ArH). ^{13}C NMR (100 MHz, $CDCl_3$) δ: 170.59, 165.85, 150.40, 136.32, 134.11, 130.36, 129.94, 129.86, 120.83.

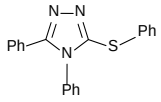

3,4-Diphenyl-5-(phenylthio)-4*H*-1,2,4-triazole (Table 3, entry 13)[6]. ^{1}H NMR (400 MHz, $CDCl_3$) δ: 8.55 – 8.53 (m, 2H, ArH), 7.56 – 7.52 (m, 1H, ArH), 7.48 – 7.43 (m, 2H, ArH), 7.32 – 7.22 (m, 8H, ArH), 7.07 – 7.04 (m, 2H, ArH). ^{13}C NMR (400 MHz, $CDCl_3$) δ: 153.07, 151.84, 150.01, 133.75, 133.64, 131.67, 130.15, 130.00, 129.79, 129.15, 128.30, 127.28, 121.44.

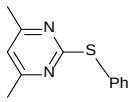

4,6-Dimethyl-2-(phenyltio)pyrimidine (Table 3, entry 14)[6]. ^{1}H NMR (300 MHz, $CDCl_3$) δ: 7.64 – 7.61 (m, 2H, ArH), 7.40 – 7.34 (m, 3H, ArH), 6.70 (s, 1H, ArH), 2.34 (s, 6H, CH_3).

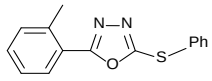

2-(Phenylthio)-5-*o*-tolyl-1,3,4-oxadiazole (Table 3, entry 15)[6]. ^{1}H NMR (400 MHz, $CDCl_3$) δ: 7.82 (d, *J* = 7.6 Hz, 1H, ArH), 7.69 – 7.67 (m, 2H, ArH), 7.44 – 7.41 (m, 3H, ArH), 7.39 – 7.36 (m,

1H, ArH), 7.30 – 7.25 (m, 2H, ArH). ^{13}C NMR (100 MHz, $CDCl_3$) δ: 166.34, 162.49, 138.71, 133.28, 132.48, 129.55, 128.73, 128.71, 127.04, 127.02, 123.72, 123.14, 21.09.

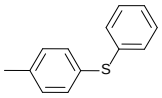

4-Methylphenyl phenyl sulfide (Table 3, entry 16)[7]. ^{1}H NMR (400 MHz, $CDCl_3$) δ: 7.28 (d, *J* = 8.4 Hz, 2H, ArH), 7.25 (m, 4H, ArH), 7.15 – 7.20 (m, 1H, ArH), 7.12 (d, *J* = 8.4 Hz , 2H, ArH), 2.34 (s, 3H, CH_3).

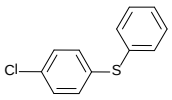

4-Chlorophenyl phenyl sulfide (Table 3, entry 17)[7]. ^{1}H NMR (300 MHz, $CDCl_3$) δ: 7.35 – 7.23 (m, 9H, ArH).

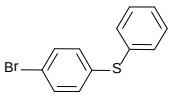

4-Bromophenyl phenyl sulfide (Table 3, entry 18)[7]. ^{1}H NMR (300 MHz, $CDCl_3$) δ: 7.51 – 7.11 (m, 9H, ArH).

5. References

[1] A. Saha, R. Kumar, R. Kumar and C. Devakumar, *J. Heterocyclic Chem.*, 2010, **47**, 838.

[2] S. Mohapatra, S. R. Rout and S. Maiti, *J. Mater. Chem.*, 2011, **21**, 9185.

[3] Z. C. Xu, C. M. Shen, Y. L. Hou, H. J. Gao and S. H. Sun, *Chem. Mater.*, 2009, **21**, 1778.

[4] S. J. Ding, Y. C. Xing, M. Radosz and Y. Q. Shen, *Macromolecules*, 2006, **39**, 6399.

[5] A. Monge-Marcet, R. Pleixats, X. Cattoen, M. W. C. Man, D. A. Alonso and C. Najera, *New J. Chem.*, 2011, **35**, 2766.

[6] L. F. Niu, Y. Cai, C. Liang, X. P. Hui and P. F. Xu, *Tetrahedron*, 2011, **67**, 2878.

[7] X. Ku, H. Huang, H. L. Jiang and H. Liu, *J. Comb. Chem.*, 2009, **11**, 338.